BULLETIN OF THE POLISH ACADEMY OF SCIENCES
TECHNICAL SCIENCES, Vol. 63, No. 4, 2015
DOI: 10.1515/bpasts-2015-0096

Pyramidal ceramic armor ability to defeat projectile threat by changing its trajectory

S. STANISLAWEK*, A. MORKA, and T. NIEZGODA

Department of Mechanics and Applied Computer Science, Military University of Technology,
2 Gen. Sylwestra Kaliskiego St., 00-908 Warsaw, Poland

Abstract. This paper presents a numerical study of a multilayer composite panel impacted by an AP (Armor Piercing) 14.5 × 114 mm B32 projectile. The composite consists of alternating layers of hard ceramic and a ductile aluminum alloy. While the alloy layer consists of typical plate, ceramics confront projectiles in the form of ceramic pyramids. The studied models are compared with a reference structure, which is a standard double layer panel.

The problem has been solved with the usage of modeling and simulation methods as well as a finite elements method implemented in LS-DYNA software. Space discretization for each option was built with three dimensional elements ensuring satisfying accuracy of the calculations. For material behavior simulation, specific models including the influence of the strain rate and temperature changes were considered. A steel projectile and aluminum plate material were described by the Johnson-Cook model and a ceramic target by the Johnson-Holmquist model.

The obtained results indicate that examined structures can be utilized as a lightweight ballistic armor in certain conditions. However, panels consisting of sets of ceramic prisms are a little easier to penetrate. Despite this fact, a ceramic layer is much less susceptible to overall destruction, making it more applicable for the armor usage. What is most important in this study is that significant projectile trajectory deviation is detected, depending on the impact point. Such an effect may be utilized in solutions, where a target is situated relatively far from an armor.

Key words: computational mechanics, ballistic protection, composite armor, ceramics.

1. Introduction

Military vehicles have been protected by armor based on steel throughout the past century. Both projectiles and various metal shields have been deeply investigated experimentally and numerically [1, 2]. The fast development of weapons and requirements for the efficient transport of vehicles to a battle field has influenced modern armor development. Mobility and speed of the vehicle is a key component of its survival in a combat situation. Nowadays, ballistic panels made of ceramics play a significant role in areas of academic and industrial activity [3, 4]. Such structures achieve better ballistic performance than projectiles due to the fact that sintered ceramics is characterized by very high hardness and compression resistance properties needed to break up a projectile. For the same ballistic protection level, areal density achieves 40–50% of the standard monolithic steel protector. However, high brittleness of ceramics makes it a great deal susceptible to cracking especially in case of multi-hit incidents [5]. To overcome such a problem ceramic tiles are often supported by an additional layer of high strength material [6]. It is also promising to create armor consisting of comparatively small components. Interesting concepts of such structures are presented in [7, 8]. Such elements can constitute any shape that is desirable for ballistic resistance with restriction only to material technology limitations.

However, a modern armor may play an additional role which is not only projectile mechanical destruction but also a more crafty way. Even if penetration occurs the vehicle body may not suffer the frontal attack due to projectile trajectory deviation. If it impacts a final target under a substantial angle it cannot utilize its basic features deciding on penetration ability [9]. Such a phenomenon is rarely investigated in nowadays literature. Moreover, it is very hard to find works in which such armors are compared with regard to their areal density. Therefore, the main aim of this paper is to investigate the ability of chosen protectors to change a projectile trajectory when their areal density is equal.

Pyramid components were chosen as elements which should cause a projectile to turn during the impact process and consequently after the bullet core perforates a target. Such components, analyzed in literature [10, 11], have relatively simple geometry, which makes them possible to manufacture in small amounts. According to numerous papers, ceramic should be backed by a solid support. For this purpose aluminum plates were used.

2. Problem solution and analysis of the results

2.1. Investigation plan. Four groups of perforation simulations have been held. Each calculation variant included the same type of a projectile and a different ballistic panel. The

*e-mail: sebastian.stanislawek@wat.edu.pl

initial speed of the heavy machine gun 14.5 × 114 mm B32 projectile, consisting of a hard core and a soft jacket, was set to 910 m/s. In order to simplify calculation, only the core of the projectile has been taken into account, assuming that the soft jacket has a negligible influence. In the reference panel (V1), the flat ceramic tile (Al_2O_3) was backed by an aluminum alloy (AA2024). In other investigated panels, the front ceramic protector consisted of a set of a closely-grained pyramids. Two layers were designed in order to protect a target from an impact in a weak point, where pyramids adjoin. In V2 variant pyramids have the same height as ceramic plate in a reference panel, while in V3 they have the same total volume. Aluminum alloy plate thickness is a result of a calculation which provides the same areal density (89 kg/m^2) for V1–V3 structures. V4 ballistic panel, used for validation tests, is very similar to variant V3, however, ceramic is covered with elastomeric material. All examined structures are depicted in Fig. 1.

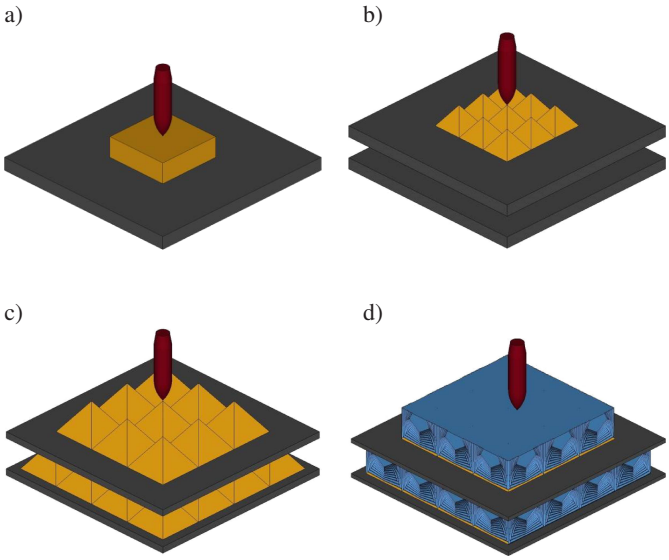

Fig. 1. Model structure: a) reference panel – V1, b) small ceramic pyramids panel – V2, c) massive ceramic pyramids panel – V3, d) massive ceramic pyramids with elastomeric filling panel – V4

Components sizes in V1 variant were selected based on preliminary calculations. They showed that target is penetrated and impact consumes around 50% of projectile energy when the thickness of ceramic and aluminum is 16 and 10 mm, respectively. It can be assumed that for other panels with similar areal density, penetration always takes place. Such an approach assures a clear comparison of projectile residual parameters both in simulation and an experimental test. The size of the components for individual variants are shown in Table 1.

Three parameters are investigated in order to verify ballistic panels' protection ability. The most important is core angular velocity which refers to trajectory deviation. The next parameter is projectile kinetic energy which is considered to be a key parameter defining core penetration ability. Finally, ceramic components' overall destruction is compared.

Table 1
Panel components dimensions

Variant number	Layer	Description
V1	1	50 × 50 × 16 mm ceramic plate
	2	150 × 150 × 10 mm aluminum alloy plate
V2	1	16 mm high ceramic prisms
	2	150 × 150 × 8.8 mm aluminum alloy plate
	3	16 mm high ceramic prisms
	4	150 × 150 × 8.8 mm aluminum alloy plate
V3	1	24 mm high ceramic prisms
	2	150 × 150 × 5 mm aluminum alloy plate
	3	24 mm high ceramic prisms
	4	150 × 150 × 5 mm aluminum alloy plate
V4	1	24 mm high ceramic prisms + elastomeric filling
	2	150 × 150 × 3 mm aluminum alloy plate
	3	24 mm high ceramic prisms + elastomeric filling
	4	150 × 150 × 3 mm aluminum alloy plate

2.2. Constitutive model and numerical method description. In order to solve the problem in an efficient way, a computer simulation method was chosen. The Finite Element Method (FEM) implemented in the LS-DYNA commercial code was used with an explicit (central difference) time integration algorithm. The boundary conditions were defined by supporting the panel at its back at a distance of 5 mm from the edges. The only initial condition was setting projectile velocity to 910 m/s. To describe the contact between ballistic panel components and projectile core, a penalty method was utilized.

All components in ballistic panels were modeled using hexagonal elements only. In the projectile, elements size was the same for whole volume, while in pyramid structures a coarser mesh was used in those (Fig. 2) components which did not interact with the projectile. In meshing the supporting plate the same idea was utilized, the mesh was denser in the central area.

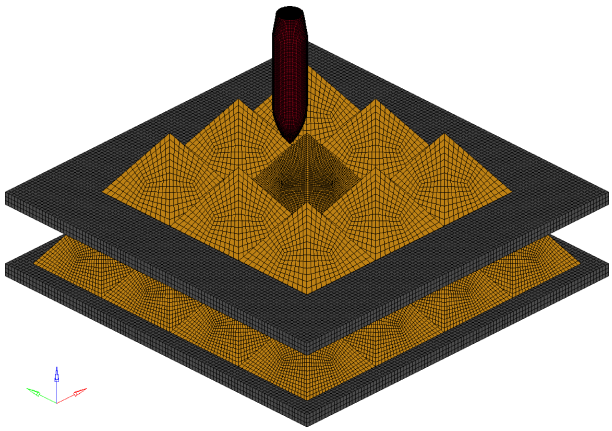

Fig. 2. Mesh utilized in V3 variant and projectile before an impact

Specific conditions of a projectile impact phenomenon require advanced material models. The projectile was made of

hard steel (HHS) while the supporting plate from aluminum alloy. In metals, yield stress needs to be defined properly. Therefore, for both metals, the Johnson-Cook model [12] was chosen:

$$\sigma = [A + B(\varepsilon_p)^n][1 + C\ln(\dot{\varepsilon}^*)][1 - (T^*)^m]. \tag{1}$$

In the above equation, A, B, C, n, m are the Johnson-Cook material behavior coefficients and:

$$T* = \frac{T - T_r}{T_m - T_r}, \qquad \dot{\varepsilon}^* = \frac{\dot{\varepsilon}_p}{\dot{\varepsilon}_0}, \tag{2}$$

where ε_p is the plastic strain, $\dot{\varepsilon}_p$ the plastic strain rate, $\dot{\varepsilon}_0$ reference strain rate, T current temperature, T_r room temperature and T_m is the melting temperature.

To characterize the plastic material behavior at high pressures the relation between the hydrostatic pressure, the local density (or specific volume), and local specific energy has been used. Isotropic part of stress tensor is described by the Gruneisen equation of state:

$$p = \left\{ \begin{array}{l} \dfrac{\rho_0 c^2 \mu[1 + (1 - \gamma_0/2)\mu - a\mu^2/2]}{\left[1 - (S_1 - 1)\mu - S_2\dfrac{\mu^2}{\mu+1} - S_3\dfrac{\mu^3}{(\mu+1)^2}\right]} \\ \qquad\qquad +(\gamma_0 + a\mu)E \ \text{ for } \ \mu \geq 0 \\ \\ \rho_0 c^2 \mu + (\gamma_0 + a\mu)E \ \text{ for } \ \mu \leq 0 \end{array} \right\}, \tag{3}$$

where ρ_0 is material initial density, ρ current density, c sound speed, S_1, S_2, S_3 constants, γ_0 Gruneisen coefficient, E internal energy per volume unit, a correction of the Gruneisen coefficient, and μ is defined by:

$$\mu = \frac{\rho}{\rho_0} - 1. \tag{4}$$

Accumulation of the damage leads to an increase of the damage parameter:

$$D = \sum \frac{\Delta\varepsilon_p}{\varepsilon^f}, \tag{5}$$

$$\varepsilon^f = [D_1 + D_2 e^{D_3\sigma^*}][1 + D_4 \ln\dot{\varepsilon}^*][1 + D_5 T^*], \tag{6}$$

where D_1, D_2, D_3, D_4, D_5 are input constants, and:

$$\sigma^* = \frac{p}{\sigma_{eff}}, \tag{7}$$

where p is pressure and σ_{eff} effective stress.

For ceramic material, the Johnson-Holmquist model [13] has been used. In such a case, equivalent stress is given in terms of the damage parameter D by:

$$\sigma^* = \sigma_i^* - D(\sigma_i^* - \sigma_f^*). \tag{8}$$

where the intact, undamaged behavior is described as:

$$\sigma_i^* = A(t^* + p^*)^N(1 + C\ln\dot{\varepsilon}^*). \tag{9}$$

While entirely destroyed material stress is

$$\sigma_f^* = B(p^*)^M(1 + C\ln\dot{\varepsilon}^*), \tag{10}$$

where A, B, C, N, M are model coefficients, and:

$$t^* = \frac{T}{p_{hel}}, \quad p^* = \frac{P}{p_{hel}}, \quad \dot{\varepsilon}^* = \frac{\dot{\varepsilon}}{\dot{\varepsilon}_0}, \quad \sigma^* = \frac{\sigma}{\sigma_{hel}}, \tag{11}$$

where T is tensile behavior of material and p_{hel} is pressure of the Hugoniot elastic limit.

The equation of state is described by:

$$p{=}k_1\mu + k_2\mu^2 + k_3\mu^3, \tag{12}$$

where k_1, k_2, k_3 are curve coefficients.

An analogical concept as for metals is utilized to describe destruction of the material. A damage parameter is calculated for each plastic deformation according to:

$$D = \sum \frac{\Delta\varepsilon^p}{\varepsilon_f^p} = 1, \tag{13}$$

where ε_f^p is plastic strain to fracture described by:

$$\varepsilon_f^p = d_1(p^* + t^*)^{d_2}, \tag{14}$$

where d_1, d_2 are input constants.

Appropriate values of material constants were presented in Table 2 and Table 3.

For validation purposes, elastomeric material was used. It may change its properties in a huge range under tensile, shear or compression load and return to its original shape. The Ogden material model [14] was used in order to describe basic properties of material where energy density is described as follows:

$$W(\lambda_1, \lambda_2, \lambda_3) = \sum_{p=1}^{N} \frac{\mu_p}{\alpha_p}(\lambda_1^{\alpha_p} + \lambda_2^{\alpha_p} + \lambda_3^{\alpha_p} - 3), \tag{15}$$

where λ_1, λ_2, λ_3 are principal strains and N, μ_p, α_p are material constants.

Table 2
Johnson-Cook constitutive model, failure model and Gruneisen equation of state data for hard steel and aluminum alloy

Parameter	Units	Hard Steel	AL2024
ρ	kg/m^3	7850	2810
T_m	K	1800	775
A	GPa	1.576	0.369
B	GPa	2.905	0.684
C		0.005	0.0083
m		0.87	1.7
n		0.117	0.73
D_1		0.0356	0.112
D_2		0.0826	0.75
D_3		−2.5	1.5
D_4		0	0.007
D_5		0	0
c	m/s	4570	5328
S_1		1.49	1.338
S_2		0	0
S_3		0	0
γ_0		1.93	0.48
a		0.5	2

Table 3
The Johnson-Holmquist constitutive model, failure model and the Gruneisen Equation of State data for alumina

Parameter	Units	Al_2O_3
ρ	kg/m^3	3890
A		0.88
B		0.45
C		0.007
m		0.6
n		0.64
T	GPa	0.462
HEL	GPa	7
BETA		1
SFMAX	GPa	1
EPSI	1/s	0.001
D_1		0.125
D_2		0.7
FS		0
k_1	GPa	231
k_2	GPa	−160
k_3	GPa	2274

The material characteristic was determined basing on laboratory tensile and compression tests and is depicted in Fig. 3.

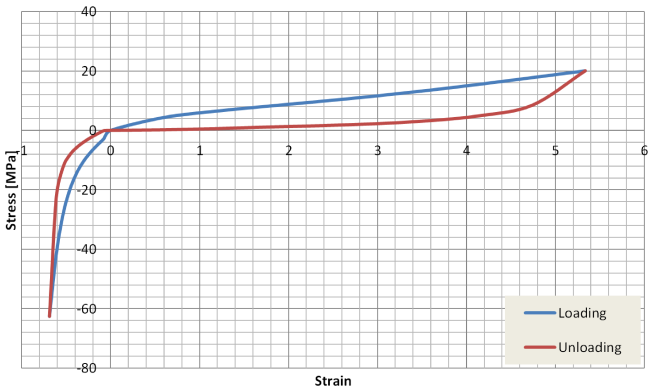

Fig. 3. Load and unload stress-strain curves for rub type material

2.3. Validation of the numerical model. Validation of the projectile and the material model was based on both theoretical analysis and experimental tests of V4 panel. The scheme of the test stand is presented in Fig. 4. The trajectory change during perforation was difficult to assess due to numerous remains of ceramic components traveling with a core. However, projectile trajectory was successfully measured.

V4 ballistic panel differs from V1–V3 panels as the ceramic-steel structure is surrounded by elastomeric material. Such a structure enabled examination of panel destruction after the experimental test because ceramic components were kept in their initial positions. Moreover, it limited an amount of debris which travelled after perforation with the projectile core. It was possible to distinguish a core shape from other objects on camera recording and asses its residual velocity. The experimental test required manufacturing a ballistic panel (Fig. 5) consisting of a set of ceramic components produced specially for this investigation.

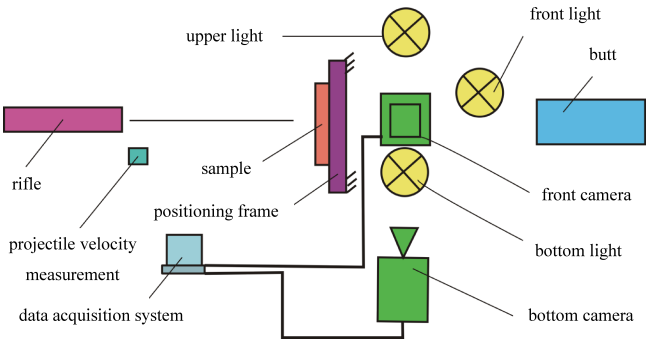

Fig. 4. Scheme of the test stand

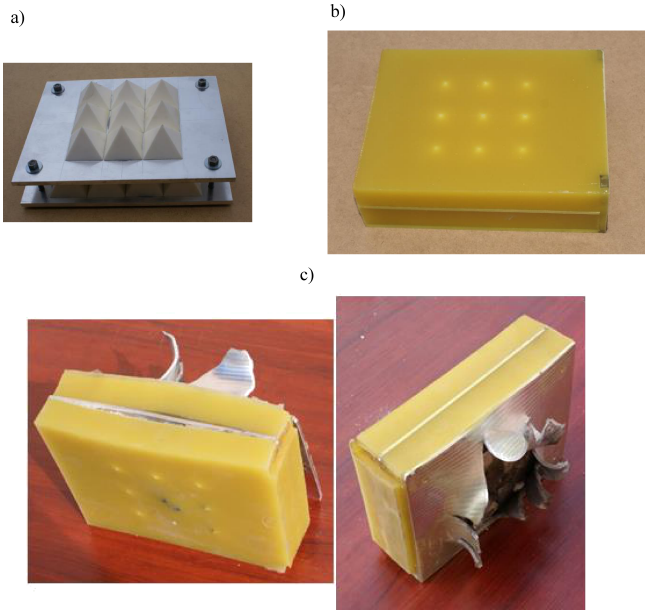

Fig. 5. Ballistic panel V4: a) before a structure was filled with elastomeric material, b) before perforation, c) after perforation

Both in simulation and an experiment the projectile has perforated ballistic panels. The initial velocity of the projectile measured during a ballistic test was 903 m/s and after impact 630 m/s ±35 m/s. Knowing the initial speed and the impact point, which is clearly seen on the specimen (Fig. 5c), boundary conditions could be properly resembled in the numerical test. The final velocity of the core was 660 m/s, which means that the applied validation procedure was successful.

2.4. Projectile trajectory deviation analyses. The main purpose of this investigation is an assessment of the composite ceramic prism's composite ability to change the 14.5 × 114 mm B32 projectile trajectory. However, considerations are not focused only on this phenomenon. While a specific armor can successfully turn the projectile, it may limit ability to resist its penetration power. Therefore, in this paper, the kinetic energy of the residual core (without taking into account the debris energy) is analyzed simultaneously. Also ceramic components'

destruction was examined in order to evaluate ballistic panel susceptibility to a multi-hit attack.

In each simulation variant, a projectile impacted in three points: at the top of the prism, its wall side and a point in which four ceramic components meet. The authors focused on those tests as they represent the thickest and the thinner section of the ceramic material. It is assumed that different impact locations will substantially influence core penetration ability and trajectory change. In Fig. 6, four stages of projectile penetration of V3 variant are shown. A substantial change in the trajectory can be observed, which takes place mainly during perforation of the first layer. While the core reaches the aluminum plate, the angle between the projectile and the ballistic panel remains almost unchanged.

In Fig. 7, projectile angular velocity is presented. In a reference variant (V1) projectile angular velocity is very low, while V3 panel presents the best properties for ceramic pyramids which have relatively big diameters allowing reaction forces to act on the core longer than in V2. Angular velocity defines both actual trajectory deviation and its value in any other time after the impact. In the case of V3 variant (side wall impact), when the core top is a distance 50 mm from the panel the angle between the projectile axis and its initial track is 20°.

Projectile residual energy for each variant is shown in Fig. 8. Shortly after perforation it becomes stable and it is clear that pyramid structures show lower ballistic resistance. V3 panel is more resistant to penetration than V2 panel, regardless of the impact point. Impacting either the prism top or the weakest point in the first layer does not change the structure's protection ability. It is caused by the fact that the examined panels consist of two prism layers, which were placed alternately. Summarizing, the obtained results indicate deterioration of panel ability to consume projectile energy while pyramid ceramic components are utilized.

Each panel was investigated in order to verify its ability to withstand a multi-hit threat. The authors believe that resistance to cracking in brittle ceramic guarantees such an ability. The cracking phenomenon described using a finite element method and erosion of the elements did not allow representation of a real shape of fractures. However, it does not dictate the way material in an impact zone is destroyed and consequently has little influence on the perforation process. A damage parameter (Fig. 9) defines the actual condition of the remaining material and may vary from zero to its maximum value unity. In such a stadium, ceramic is considered to be completely grained. It gives us a rough idea of how the ceramic components would look after the ballistic test. Based on the simulation results, cracking of the pyramid structure does not transfer to adjacent components.

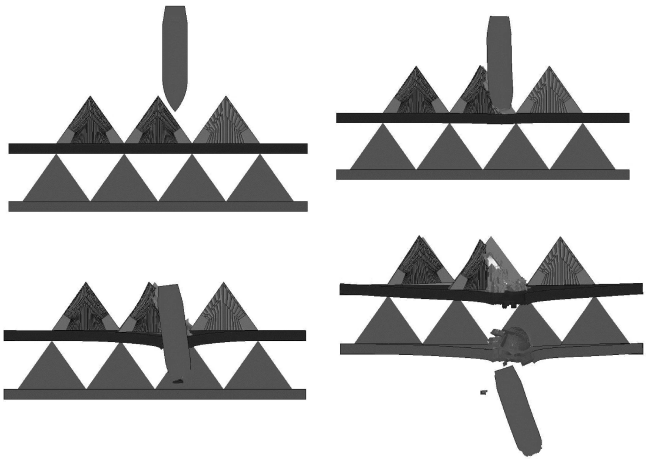

Fig. 6. Four stages of projectile penetration for V3 variant (cross section)

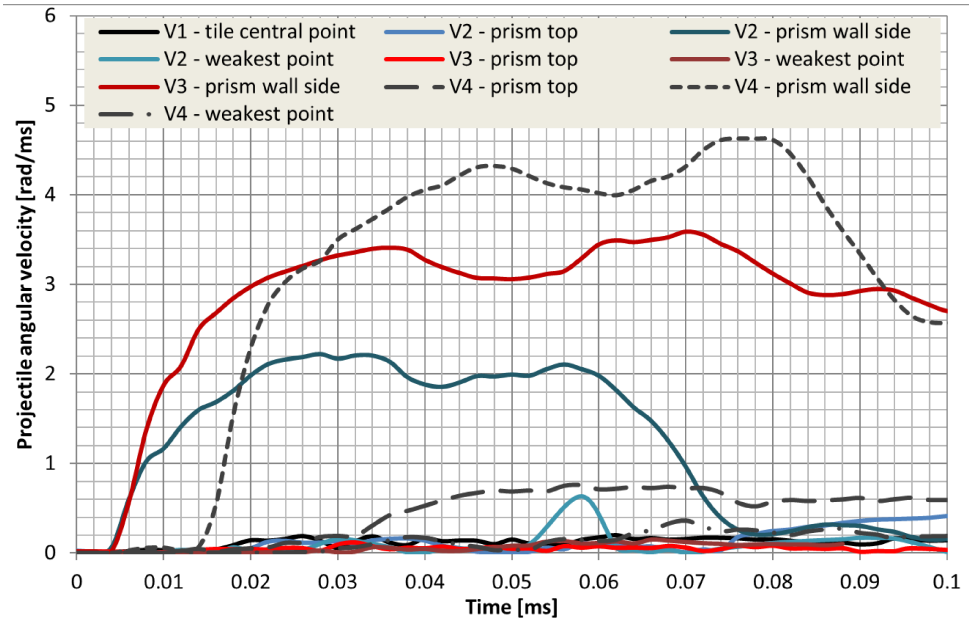

Fig. 7. Resultant angular velocity of the core for different panel type and three impact points

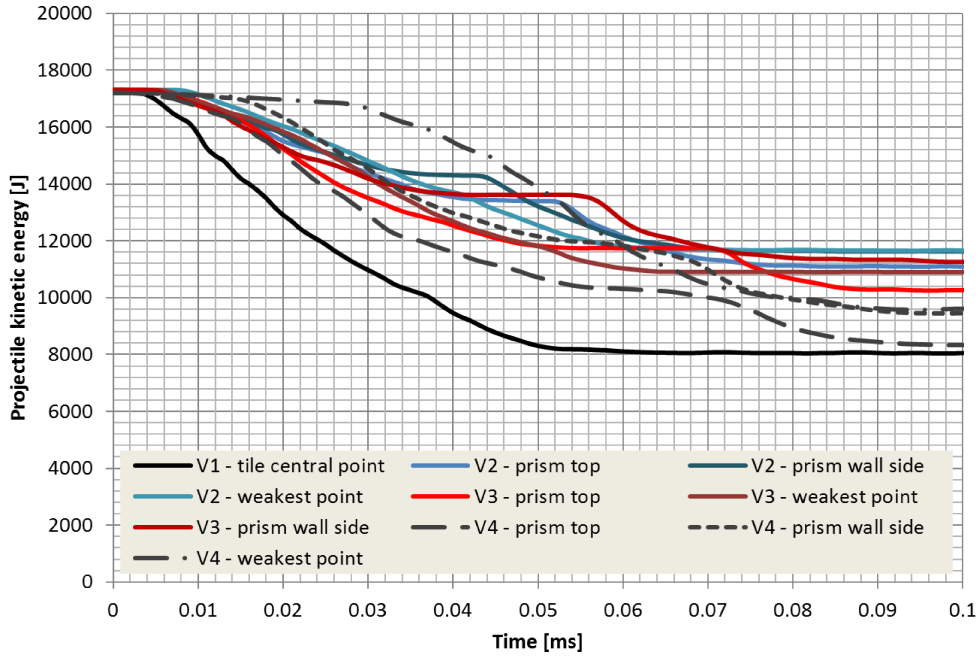

Fig. 8. Kinetic energy of the core for three type of panels and three impact points

a) b)

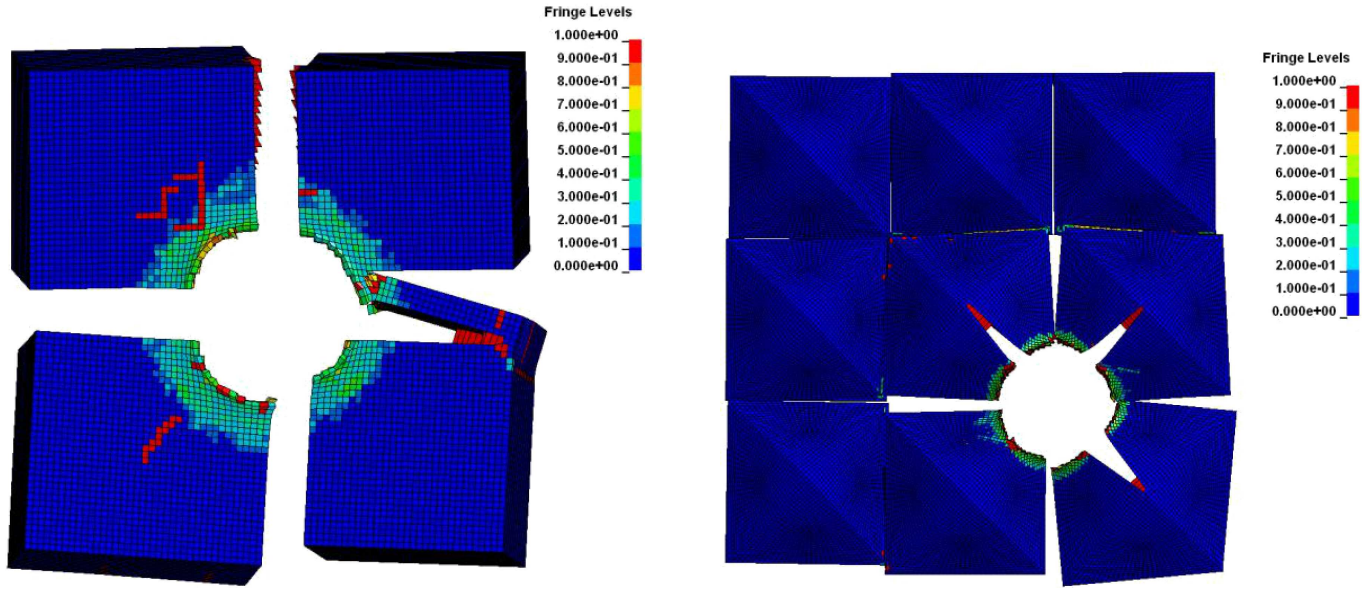

Fig. 9. Destruction parameter in ceramic material: a) reference panel V1, b) front layer of V2 panel

3. Conclusions

The obtained results indicate that a pyramidal ceramic armor can defeat a projectile threat by changing its trajectory. The investigation has proved that the projectile core turns as a result of ceramic component impact. Such a phenomenon is observed especially in situations where pyramids have relatively big dimensions and an impact point is situated on a pyramid side wall. However, the described effect can be utilized in solutions, where a target is situated relatively far from an armor. Such a limitation is caused by the fact that projectile angular velocity observed during the penetration process is not very high. A vehicle body must be enough distant from an armor to allow a projectile to change its trajectory substantially.

Another issue is a ballistic panels energy consumption ability. Unfortunately, panels consisting of sets of ceramic prisms are up to 28% easier to penetrate. Despite this fact, a ceramic layer is much less susceptible to overall destruction, which makes it more applicable for armour usage.

The investigated panels are currently only academic structures. The question arises as to whether they could be used as real protection for modern vehicles. Most available ballistic

ceramic components are in various sizes, however, they are mainly in the form of tiles. However, looking into an abrasive products field, it becomes obvious that the cost of ceramic prisms is only a matter of quantity but not a technological barrier. Further studies should be carried out in order to examine an influence of different ceramic component geometry as well as the backing thickness in order to find the best possible solutions.

REFERENCES

[1] T.J. Holmquist and C.L. Randow, "Modeling the ballistic response of the 14.5 mm BS41 projectile", *Eur. Phys. J. Special Topics* 206, 129–137 (2012).

[2] T.J. Holmquist, G.R. Johnson, and W.A. Gooch, "Modeling the 14.5 mm BS41 projectile for ballistic impact computations", *Computational Ballistics II, WIT Trans. on Modelling and Simulation* 4, 61–75 (2005).

[3] A. Bhatnagar, *Lightweight Ballistic Composites: Military and Law-Enforcement Applications*, Woodhead Publishing Ltd., Michigan, 2006.

[4] P. Chabera, A. Boczkowska, A. Morka, P. Kędzierski, T. Niezgoda, A. Oziębło, and A. Witek, "Comparison of numerical and experimental study of armour system based on alumina and silicon carbide ceramics", *Bull. Pol. Ac.: Tech.* 63 (2), 363–367 (2015).

[5] E. Medvedovski, "Ballistic performance of armour ceramics: Influence of design and structure. Part 2", *Ceramics Int.* 36, 2117–2127 (2010).

[6] P. Kędzierski, A. Morka, G. Sławiński, and T. Niezgoda, "Optimization of two-component armour", *Bull. Pol. Ac.: Tech.* 63 (1), 173–179 (2015).

[7] J. Jovicic, A. Zavaliangos, and F. Ko, "Modeling of the ballistic behavior of gradient design composite armors", *Composites Part* A 31, 773–784 (2000).

[8] C.Y. Nia, Y.C. Lib, F.X. Xina, F. Jina, and T.J. Lu, "Ballistic resistance of hybrid-cored sandwich plates: numerical and experimental assessment", *Composites Part* A 46, 69–79 (2013).

[9] M. Wilkins, "Mechanics of penetration and perforation", *Int. J. Eng. Sci.* 16, 793–807 (1978).

[10] D.L. Hunn and S.J. Lee, "Development of a novel ceramic armor system: analysis and test", *26th Int. Symp. Ballistic* 1, 12–16 (2011).

[11] C.J. Yungwirth, D.D. Radford, M. Aronson, and H.N.G. Wadley, "Experiment assessment of the ballistic response of composite pyramidal lattice truss structures composite pyramidal lattice truss structures", *Composites Part* B 39, 556–569 (2008).

[12] G.R. Johnson and W.H. Cook, "A constitutive model and data for metals subjected to large strains, high strain rates and high temperatures", *Proc. 7th Int. Symp. Ballistics* 1, 541–547 (1983).

[13] G. McIntosh, *The Johnson-Holmquist Ceramic Model as Used in LS-Dyna 2D*, Defence Research Establishment, Quebec, 1998.

[14] P.A. Du Bois, "A simplified approach to the simulation of rubber-like materials under dynamic loading", *4th Eur. LS-DYNA Users Conf.* 1, CD-ROM (2003).